Published November 1, 2018

Special Section: Advancing Soil Physics for Securing Food, Water, Soil and Ecosystem Services

Core Ideas

- The cumulative infiltration decreased with increasing soil water repellency.
- Soil water movement in higher water-repellent levels tended to be more unstable.
- Finger flow occurred preferentially in the coarser, more water-repellent soils.
- Strong correlations of cumulative infiltration and cumulative wetting area were shown.

Water Movement and Finger Flow Characterization in Homogeneous Water-Repellent Soils

Yichen Wang, Xiaofang Wang, Henry Wai Chau, Bingcheng Si, Ning Yao, and Yi Li*

Soil water repellency (SWR) is a widespread property in soils around the world. It influences soil water movement and causes unstable flow. The mechanics of finger flow occurrence in water-repellent soils are not clearly understood. Slab chamber infiltration experiments consisting of increasing SWR persistence in clay and sandy loam soils were conducted to compare wetting front advancement and mechanics of finger flow development. The temporal variation curves of cumulative infiltration (CI) decreased with an increase in SWR persistence. For wettable soils, the wetting front advanced regularly with time, but for water-repellent soils, it became unstable and finger flow occurred as the SWR persistence increased. Water movement in soils with higher SWR persistence tended to be more unstable. Water repellency contributed to finger flow development, especially for sandy loam. There were strong correlations among CI, finger length, and the cumulative wetting area. In the strongly, severely, and extremely water-repellent sandy loam soils, the power function relationship fit better than the linear function. The average soil water content decreased with a higher SWR persistence, which meant that less water was available in the profile. Finger flow development was related to the more severe water-repellent conditions and tended to be more easily formed in the water-repellent sandy loam soils than the clay loam soils due to the faster infiltration rate.

Abbreviations: DCDMS, dichlorodimethylsilane; SWR, soil water repellency; WDPT, water droplet penetration time.

Y. Wang, X. Wang, N. Yao, and Y. Li, College of Water Resources and Architectural Engineering, Northwest Agriculture and Forestry Sci-Tech Univ., Yangling 712100, China; Y. Wang, Beijing Hydrology Center, Beiwaxili No. 51, Haidian, Beijing 100089, China; H.W. Chau, Dep. of Soil and Physical Sciences, Faculty of Agriculture and Life Science, Lincoln Univ., Lincoln, Canterbury, 7647, New Zealand; B. Si, Univ. of Saskatchewan, Saskatoon, SK S7N3H5, Canada. Y. Wang and X. Wang contributed equally to this work. *Corresponding author (liyikitty@126.com).

Received 27 Jan. 2018.
Accepted 10 Aug. 2018.

Citation: Citation: Y. Wang, X. Wang, H.W. Chau, B. Si, N. Yao, and Y. Li. 2018. Water movement and finger flow characterization in homogenous water-repellent soils. Vadose Zone J. 17:180021. doi:10.2136/vzj2018.01.0021

Soil water repellency (SWR) is a phenomenon describing a delayed or reduced infiltration of water into soil (Dekker and Ritsema, 1994). It is a ubiquitous property and can be found in different regions of the world in all types of climates (DeBano, 1981; Li et al., 2017). Soil water repellency alters hydrological and geomorphological processes; affects spatiotemporal dynamics of soil water movement by generating unstable and preferential flow, which accelerates the transport of water and solutes; and increases the groundwater contamination risk and loss of crop yield (Dekker and Ritsema, 1994; Ganz et al., 2013b). Many studies have highlighted that SWR is a concern in soils for efficient water utilization (DeBano, 1981; Dekker and Ritsema, 1994; Li et al., 2017). Urbanek and Doerr (2017) suggested that spatial variability in SWR and associated soil moisture distribution needs to be considered when evaluating the effects of SWR on soil carbon dynamics under current and predicted future climatic conditions. Zheng et al. (2017) analyzed SWR influences on the hydrological response of natural and man-made slopes at angles of 20 and 40°, and relative compactions of 70 and 90%. They concluded that an increase in SWR reduced infiltration, shortened runoff generation time, and amplified high rainfall intensity.

Finger flow is a dominant form of preferential flow. The initially planar wetting front breaks up into wetting columns, called preferential flow paths or fingers (de Rooij, 2000). Finger flow has an irregular and special wetting front shape through which water moves nonuniformly as fingers (Rezanezhad et al., 2006). Subsequently, infiltration and the soil water distribution are affected. It can occur either in structured or homogeneous soils (Ritsema et al., 1997). Finger flow formation can be driven by heterogeneity or instability.

The former type of fingers generally occurs in clay and peat soils with well-defined macropore or mesopore networks. Although instability-driven fingers have been found in water-repellent soils (Ritsema and Dekker, 1994, 2000; Bauters et al., 1998; Carrillo et al., 2000a). There are many factors that induce finger-like pathways, including hysteresis (Ritsema et al., 1998), SWR, soil structure, different head pressures on the soil surface from a point source water application (Wallach and Jortzick, 2008), and so on. For the research related to the influence of SWR on finger flow development, Ritsema and Dekker (1994) found that fingers preferred to form in the places where the top layer had the lowest degree of potential SWR. Carrillo et al. (2000a) conducted laboratory infiltration experiments with different water entry pressures in the top layer. They found that with the increase in water droplet penetration time (WDPT) (DeBano, 1981), the tendency for finger formation also increased. Wallach and Jortzick (2008) observed finger-like wetting fronts during point-source infiltration in the wettable and water-repellent sands, and they found that the horizontal wetting front in water-repellent soils did not obey the horizontal capillary-dependent flow theory. Ganz et al. (2013a) concluded that the wettability characteristics in a sandy soil with low SWR might be relevant for assessing infiltration dynamics at other sites.

Along the profiles, persistent SWR was responsible for a conical plume geometry (Ganz et al., 2013b). Wang et al. (2003) showed that the variability in infiltration rate in layered water-repellent soils was contrary to wettable homogeneous soils. Li et al. (2018) found that the SWR persistence of a silt loam layer had a greater effect on infiltration than the layer position. Sepehrnia et al. (2017) concluded that SWR affected moisture distribution and resulted in the upper layer (0–40 cm) of water-repellent soil being considerably drier than wettable soil. Rye and Smettem (2017) found that SWR increased the maximum pathway depth of water movement due to finger flow.

Although previous research has explained the generation of preferential flow in water-repellent soils, there are difficulties in understanding finger flow patterns in water-repellent soils. For example, few studies have quantified the finger flow patterns in water-repellent soils. Some SWR-related questions remained unclear (e.g., how has the soil texture changed how the infiltration rate (*i*) and cumulative infiltration (CI) vary, and what is the quantitative relationship between wetting front distances and wetting area in such soils). These questions still have not been answered because of the complexity of interactions between the soil water movement and SWR. Our objectives are (i) to analyze different infiltration parameters and their quantitative connections and to investigate the infiltration feature differences for two homogeneous water-repellent soils; (ii) to reveal the effects of SWR on soil water movement when unstable flow has occurred; and (iii) to generalize two soil textures of clay loam and sandy loam, SWR persistence conditions, and mechanics that cause finger flow development in homogeneous WR soils. To achieve these aims, water infiltration experiments were performed in a clay loam and sandy loam soil with increasing SWR persistence. The finger flow (if it occurs) and infiltration parameters including CI, *i*, finger length (F_L), width of half finger (FW_h), wetting front velocity (F_v), and volumetric soil water content (θ_v) were quantified and compared with increasing SWR persistence. The findings of this study will improve the conceptual understanding of finger flow development in water-repellent soils.

Materials and Methods

Soils

Soil samples from two types were collected from the top 0- to 30-cm depth of a corn (*Zea mays* L.) field and Wei riversides in Yangling, Shaanxi, China. After the removal of crop residues and passing the samples through a 2-mm-diam. sieve, the soils were air dried for the laboratory soil chamber experiments. The particle contents were measured using a laser diffractometry (long bench Mastersizer 2000, Malvern Instruments). Soil textures were classified according to the International Classification System (Table 1). The gravimetric soil water content (θ_g) was measured using the oven-drying method. The soil samples were put into an oven at 105°C for 10 h.

The WDPT test was used to measure SWR persistence (Dekker and Jungerius, 1990). Water droplets (0.05 mL) were placed onto the soil surface and were recorded until the water infiltrated into soils. For each sample, the average WDPT value of eight replicate water droplets was used for its persistence. Soils with WDPT <5 s are wettable (DeBano, 1981). The scale used to classify WDPT values ranges from 6 to 59 s for slightly water repellent, 60 to 599 s for strongly water repellent, 600 to 3600 s for severely water repellent, and >3600 s for extremely water repellent (Bisdom et al., 1993). The average WDPT values of eight replicates were used to determine the initial WDPT of the two air-dried soils (Table 1). The two types of soils collected were initially wettable.

Dichlorodimethylsilane (DCDMS), a transparent oil-like liquid, can encapsulate soil particles. It is a common and effective chemical that reacts with water and produces polydimethylsiloxane

Table 1. Physical properties† of the sampled wettable soils.

Soil	Clay	Silt	Sand	θ_r	θ_s	K_s	BD	$WDPT_i$
	%			cm cm^{-3}		cm min^{-1}	g cm^{-3}	s
Clay loam	18	42	40	2.50×10^{-2}	0.46	6×10^{-4}	1.4	1.5 ± 0.3
Sandy loam	7	23	70	3×10^{-3}	0.36	5.40×10^{-2}	1.7	0.5 ± 1.2

† θ_r, air-dried soil water content; θ_s, saturated soil water content; K_s, saturated hydraulic conductivity; BD, bulk density; $WDPT_i$, water droplet penetration time of non-dichlorodimethylsilane-treated soil samples. The range of particle diameters for clay, silt, and sand are <0.002, 0.002 to 0.02, and 0.02 to 2 mm, respectively, following the International Classification System.

and HCl (Goebel et al., 2007) and forms a relatively stable hydrophobic layer outside of the soil particles and creates stable and persistent water-repellent soils (Bachmann and van der Ploeg, 2002). The DCDMS was added to the prepared wettable clay loam and sandy loam gradually. After saturation with distilled water, the soils were mixed uniformly. Then, the soils were air dried and left to reach equilibrium to achieve stable and persistent SWR. For the DCDMS application amounts, the tested WDPT ($WDPT_p$) and the contact angle (ω) values using average of eight replications (following Bachmann and van der Ploeg, 2002) of the prepared water-repellent clay loam and sandy loam soils are given in Table 2. The different SWR persistence treatments of chamber infiltration experiments and the representing names of all treatments are also given in Table 2.

Cuboid soil chambers, made of transparent Plexiglas, were used for the observations during the infiltration. The chambers had a wall thickness of 0.8 cm and a volume of 60 × 45 × 5 cm. To avoid water leakage, Vaseline was applied on each edge and connecting points. The air-dried wettable and water-repellent soils were packed into the container to 55-cm depth with the bulk density listed in Table 1. Then, the containers were left for a 24-h soil-settling period. Two soil groups of clay loam and sandy loam (abbreviated as CL and SL in treatment names, respectively), which had a changing SWR persistence, were termed as WET, WR1, WR2, WR3, and WR4 corresponding to wettable, slightly water repellent, strongly water repellent, severely water repellent, and extremely water repellent, respectively. For example, SLWR1 means the treatment of slightly water-repellent sandy loam. A total of 10 treatments were designed (Table 2). Three replications were conducted for each treatment.

Table 2. The basic properties of the prepared water-repellent soils.

DCDMS† application	$WDPT_p$‡	Soil water repellency persistence	ω§	Treatment
g kg^{-1}	s		°	
		Clay loam		
0	0.65 ± 0.09	wettable	0	CLWET
16.2	40.6 ± 13.4	slightly water repellent	105 ± 2.5	CLWR1
24.3	83.2 ± 21.1	strongly water repellent	116 ± 9.1	CLWR2
48.6	1854 ± 262	severely water repellent	129 ± 8.3	CLWR3
64.8	4308 ± 521	extremely water repellent	138 ± 10.2	CLWR4
		Sandy loam		
0	0.18 ± 0.10	wettable	0	SLWET
24.3	27.8 ± 5.80	slightly water repellent	99 ± 2.6	SLWR1
32.4	312 ± 88.3	strongly water repellent	108 ± 3.8	SLWR2
64.8	1009 ± 111	severely water repellent	112 ± 12.3	SLWR3
72.9	4008 ± 120	extremely water repellent	117 ± 8.8	SLWR4

† DCDMS, dichlorodimethylsilane.
‡ $WDPT_p$, water droplet penetration time for DCDMS-treated soils.
§ ω, contact angle.

Infiltration Experiment

A total of 30 ponded infiltration experiments for the 10 treatments were conducted (Fig. 1). A Mariotte bottle with distilled water was connected to the soil chamber to maintain a constant water depth of 2 cm on the soil surface, which was padded with filter papers to prevent water scouring and soil splashing.

The wetting processes during infiltration were traced using Brilliant Blue FCF dye with a concentration of 20 g m^{-3} in distilled water. At this concentration, soil water movement was affected minimally and the wetting fronts were observed clearly. Cumulative infiltration (CI) was measured by the water table changes from the Mariotte bottle at different times. The advances of wetting front were marked on the container walls for different infiltration stages. To avoid the influences of the lower boundary, the experiments were stopped when the wetting front reached 45 cm. When the infiltration terminated, one of the chamber walls was loosened and soil samples were taken one after another as soon as possible to measure θ_g using the oven-drying method. Soil samples of the wetting zones were taken at a 5-cm by 5-cm grid interval along the soil chamber wall, and θ_v was determined by multiplying by the bulk density.

Data Analysis

Different finger flow properties were obtained based on the measurement, including CI, wetting front, cumulative wetting

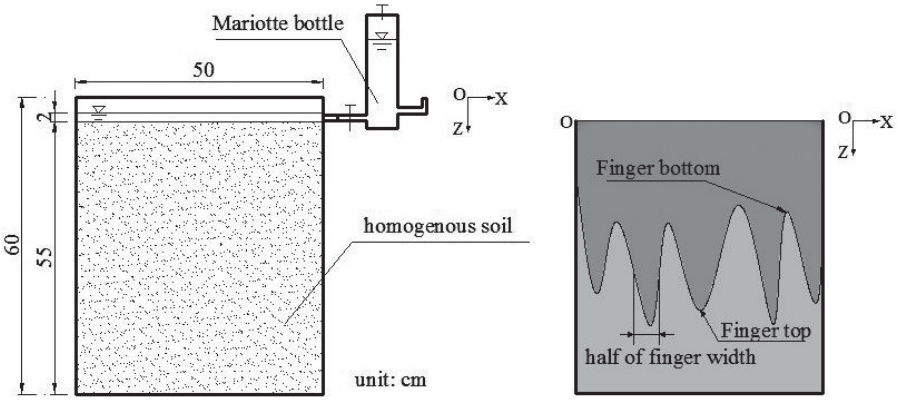

Fig. 1. The experimental equipment and sketch of finger flow. *O* is the origin of the coordinate system, *X* is the horizontal axis, and *Z* is the vertical axis.

area (WA, cm^2), F_L (i.e., the length from finger bottom to finger top, cm), FW_h (cm), and finger front velocity F_v (i.e., finger top movement distance in unit time, cm s^{-1})

The shape index (SI) and distributing index (DI) were calculated by F_L and FW_h (Zhang, 2004):

$$SI = \frac{F_L}{FW_h} \quad [1]$$

$$DI = \sqrt{\frac{1}{N}\sum_{k=1}^{N}\left|F_{L,k} - \overline{F}_L\right|} \quad [2]$$

where $F_{L,k}$ is F_L of the kth finger (k = 1, 2, ..., N), N is the total number of fingers, and $\overline{F}_L$ is the average value of F_L.

The variability extents of SI and DI were quantified with the CV, calculated with the following equation (Nielsen and Bouma, 1985):

$$CV = \sigma/\overline{x} \quad [3]$$

where σ is the SE and $\overline{x}$ is the average of x series. The ranges of $CV \leq 0.1$, $0.1 < CV < 1.0$, and $CV \geq 1.0$ were classified as weak, moderate, or strong variability.

Considering strong variability and randomness of finger flow, three replicates for the 10 treatments were conducted. The occurrence of finger flow and its movement was very random. In our experiments, only the three replications of the CLWET, SLWET, and CLWR treatments had similar wetting fronts. When comparing CI, i, and WA, much smaller variability was observed. Considering the random nature of preferential flow, these differences cannot be masked by adding replications. The differences of wetting front and soil moisture among the three replications may also partially due to water-repellent soils being configured by adding certain amounts of DCDMS. Still, three replications can generally describe the finger development characteristics.

SigmaPlot 12.5 (Systat Software, 2013) was used to plot the figures. The contour maps of θ_v were completed in the Surfer 11.0 software (Li et al., 2013). Excel 2007 was used to calculate finger flow indices. SPSS 17.0 (SPSS, 2008) was used for statistical analysis.

Results and Discussion

Cumulative Infiltration

The variations in CI and i vs. time for the 10 water-repellent soil treatments are illustrated in Fig. 2 (with error bars generated from the three replications). Figure 2 shows that the CI curves generally decreased with the increasing of SWR persistence for both clay loam and sandy loam soils. At the same level of SWR persistence, CI and i differed for both clay loam and sandy loam soils; however, soil with finer texture showed a slower water infiltration as expected. Soils with coarser textures have larger pore diameters, resulting in the larger i values. The initial values of i decreased with the increasing SWR persistence. The influence of texture on infiltration was observed and was also indicated by other research. For example, Li et al. (2018) reported that CI and i values were larger in wettable sand than in the silt loam, and a larger i was observed in the silt loam overlying sand conditions than in the sand overlying silt loam layered conditions, as the SWR persistence varied. In the clay loam soil, i decreased with time during the entire infiltration and reached a steady i after 120 min (Li et al., 2018). Figure 2 also shows that the i values decreased with the increase of the SWR persistence. However, the i vs. time curves of treatments SLWR1, SLWR2, SLWR3 and SLWR4 increased with time. The i vs. time curve increase followed a decreasing order with the increasing SWR persistence. Different from the other four treatments, only the wettable sandy loam treatment SLWET had a fast decrease in the i vs. time curve. Instability and finger flow occurred in the treatments of SLWR1, SLWR2, SLWR3, and SLWR4, which may lead to unexpected fast water movement in some unknown paths.

Song et al. (2014) named the increase of i during longer infiltration in water-repellent soils as "rewettability." They compared the effects of six wetting agents on sand rewettability. They found that the i increase at the later time during the infiltration process, which was characteristic of water-repellent soils. Wang et al. (2003) also found a gradually increased infiltration rate or rewettability in infiltration of water-repellent soils. Deurer and Bachmann (2007) reported rewettability along a transect at the top of the root zone. They concluded that the more persistent the SWR, the smaller the increase of i into the root zone. Robichaud et al. (2016) investigated infiltration rates of wildfire-induced ash cap soils, which were water repellent 0, 1, 2, and 5 yr after fire. From their results, i decreased rapidly within the initial 5 min for all of the treatments. It was stable or showed slight rewettability for the treatments 1 and 2 yr after fire. Carrillo et al. (2000b) showed that the water i increased with time and then plateaued, which agreed partially with our results for rewettability occurrence in sandy loam, implying a breakthrough of SWR when infiltration lasted longer.

Wetting Front Variations

The wetting front advances and finger flow development for the three replications of 10 treatments for both clay loam and sandy loam are illustrated in Fig. 3. In treatments CLWET, SLWET, and CLWR1, soil water movement was close to being homogeneous and the three replications were generally consistent. With increasing SWR persistence, wetting fronts became increasingly unstable and irregular.

In treatments SLWET, CLWR1, and CLWR2, no obvious finger was developed but the wetting fronts were not as uniform with that of the wettable clay loam as time increased. For treatments CLWR3, (one replication of) CLWR4, and SLWR1, discontinuous wetting fronts were observed, water flowed through preferential flow paths, and wetting fronts became unstable. For (three replications of) CLWR4, SLWR2, SLWR3, and SLWR4, fingers formed at infiltration times of 110 to 156, 17 to 19, 20 to 24, and 22 to 56 min, respectively. Therefore, water repellency extended the time for finger flow to occur depending on both SWR persistence and soil texture. Therefore, fingers were discontinuous or connected with invisible

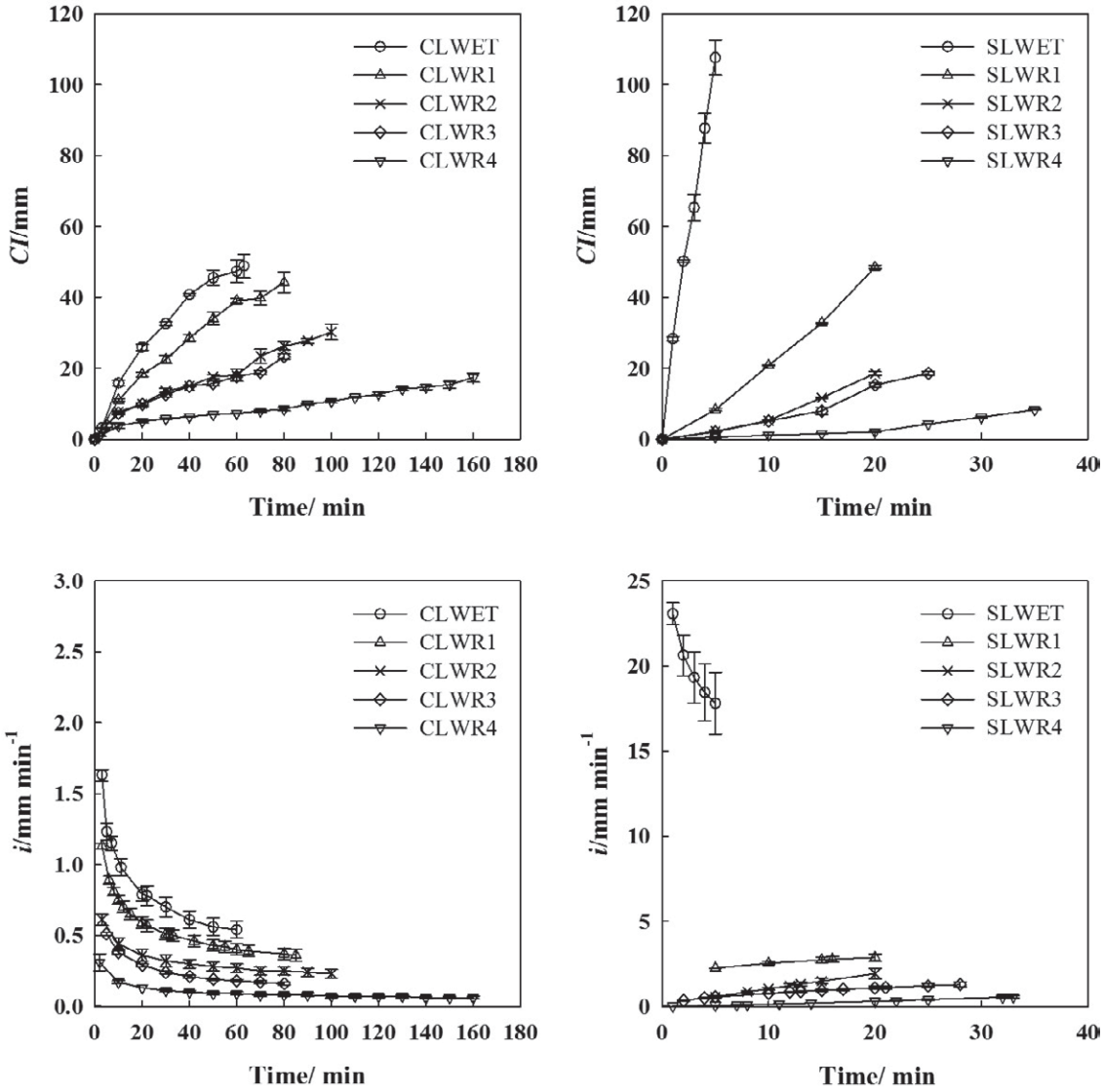

Fig. 2. Temporal variations of cumulative infiltration (CI) and infiltrating rate (i) with error bars generated from the three replications for the 10 treatments. See Table 2 for treatment abbreviation definitions.

unknown paths. Unstable flow occurred for both soil textures, but fingers developed much faster and at higher SWR persistence for the sandy loam soils, which meant that SWR may cause finger flow development but decreases the infiltration rate. In addition, finger number and finger interval differed for three replications of the same treatment, showing certain variability and randomness of finger flow. Nevertheless, wetting front is a rather apparent index compared with CI.

Kramers et al. (2005) found that the size of the preferential flow in the soil profile depends on several factors such as the weather history, the soil textural heterogeneity, the spatial distribution of SWR, and the interaction between these factors. Carrillo et al. (2000a) conducted experiments in a specially built rectangular chamber on water-repellent sand layers that had WDPT values of 1, 10, and 150 min. The authors stated that the formation of finger water flow was related to WDPT of the layer and the ratio of $h_0 + L$ (depth to the water-repellent layer plus the depth of ponded water) to water entry pressure. Carrillo et al. (2000b) confirmed that an increase in this ratio is due to increasing thickness of the fingers for the high-WDPT (150 min at extreme SWR) treatment. More detailed information is needed to reveal instability or finger flow development characteristics. Several broken fingers were observed in this research, whereas smooth and continuous fingers were observed in Carrillo et al. (2000a, 2000b). The difference in finger shapes between previous research and this study may be connected to changes in soil type and SWR persistence.

Wetting Area Variations and Relationships with Cumulative Infiltration

For all 10 treatments (averaged from three replicates), WA increased with increasing time (Fig. 4a). Since CI increased with time, WA also increased with the increasing CI (data were averaged from three replicates, Fig. 4b). For CLWET and SLWET,

WA generally increased with CI almost linearly. For the three CLWR treatments, WA increased with CI exponentially. For the four CLWR treatments, WA increased slowly with the increase of CI, which may be due to more water moving through the finger flow paths, including some invisible wetting areas in the soils, implying that more water passed a limited soil area as the SWR persistence increased. However, in the CLWR4 treatment, WA was larger than the four water-repellent treatments of sandy loam. A universal power function was fitted between WA and CI for all the treatments with high R^2 (>0.97, Table 3).

Carrillo et al. (2000b) also agreed that as time progressed, a larger fraction of area was wetted. Hardie et al. (2011) studied preferential flow in the texture-contrasting soils and indicated a decreased proportion of dye stained in soil along the vertical profile. However, the quantitative relationship of CI and WA was seldom studied before. Our study investigated the changes of F_L

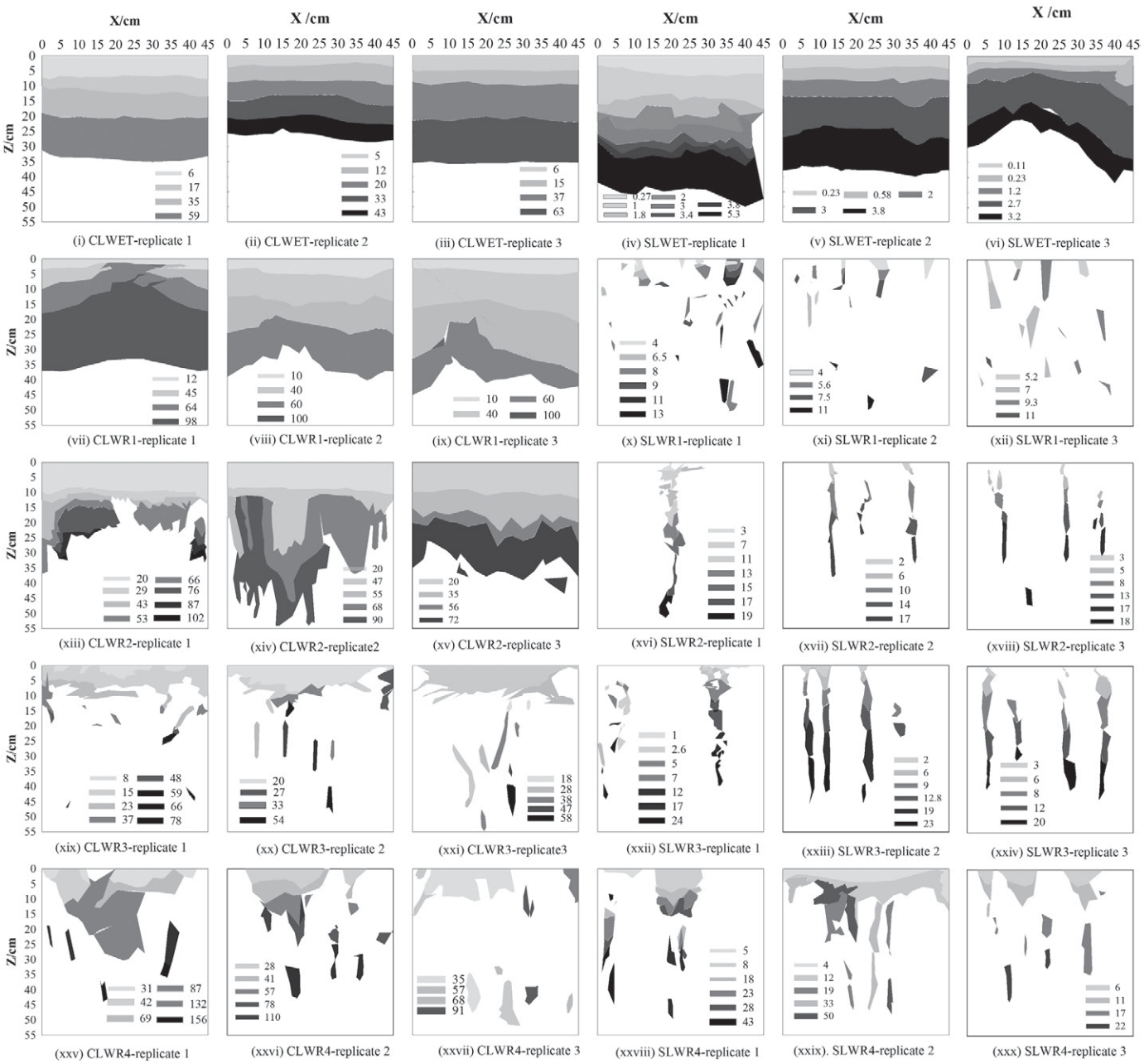

Fig. 3. Wetting front movement of three replicates of the 10 treatments for clay loam (CL) and sandy loam (SL) soils. The legends denote infiltration time (min). The darker the shade, the longer the infiltration time. See Table 2 for treatment abbreviation definitions. *X* is the horizontal axis and *Z* is the vertical axis.

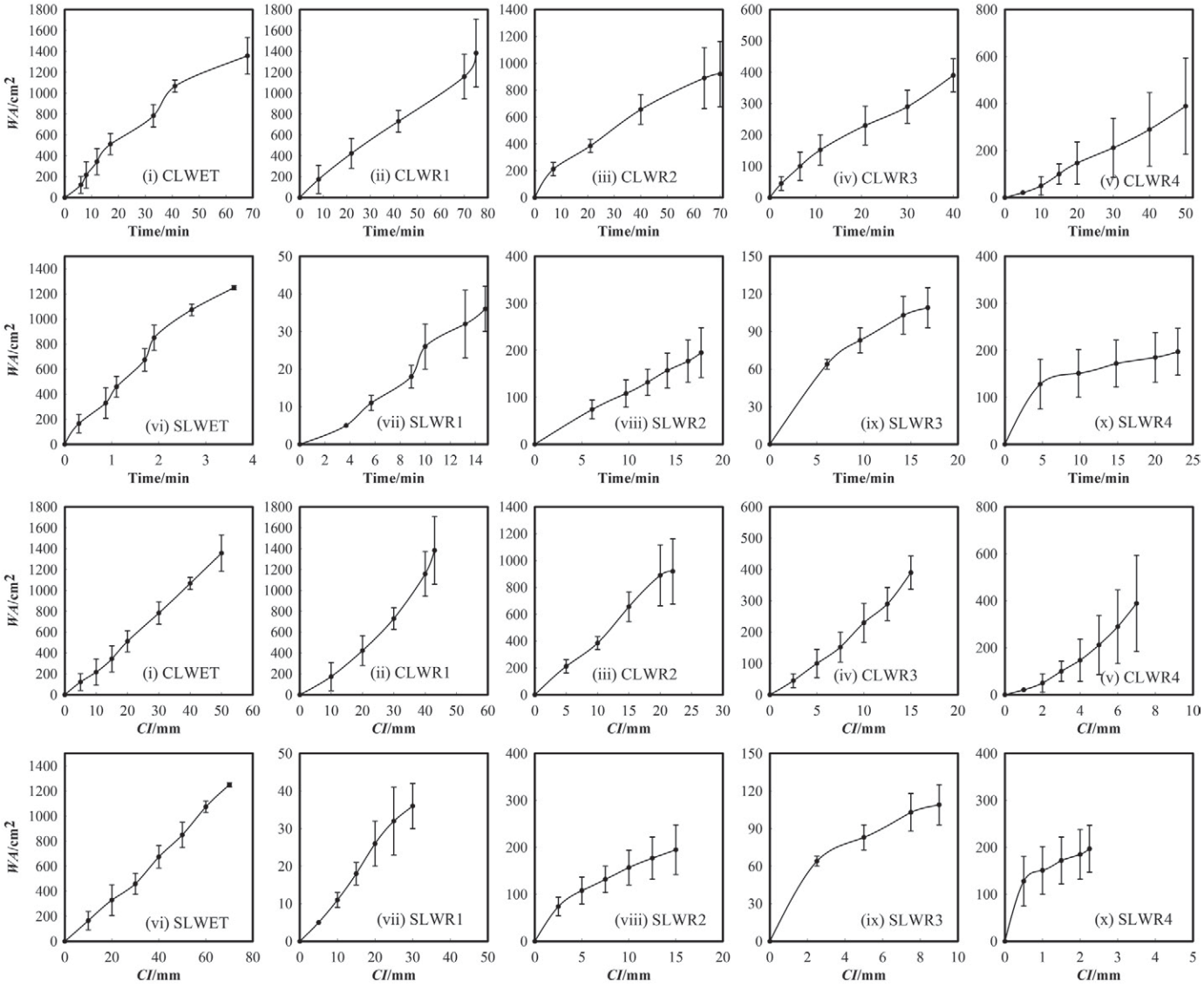

Fig. 4. Curves of (a) wetting area (WA) variation with time and (b) cumulative infiltration (CI) × WA of the 10 treatments. Averages values for three replications were used, and error bars are indicated. See Table 2 for treatment abbreviation definitions.

for two types of homogeneous water-repellent soils and quantitatively related CI to WA.

Finger Flow Characteristics

As shown in Fig. 2, a wide finger occurred in two replicates of CLWR4, and several fingers were observed in SLWR2, SLWR3, and SLWR4. To further investigate the effects of SWR on finger flow, the minimum, average, and maximum values (calculated first based on each finger and then averaged for all of the fingers occurring in the same replication) of finger number, F_L, FW_h, SI, and DI for treatments CLWR4, SLWR2, SLWR3, and SLWR4 are given in Table 4. Finger parameters (from different replications of each treatment) varied with randomness but were still related to SWR persistence to a great extent for SLWR2, SLWR3, and SLWR4. In treatment SLWR4, the maximum F_L reached the largest value of 45.7 cm, and FW_h also reached the largest value of 4.0 cm. Although fingers were not universally connected, they were visible on both sides, indicating that they were connected through an inner pathway. As SWR persistence changed from strongly to extremely repellent for sandy loam, the minimum, average, and maximum values of F_L and FW_h consistently increased with the increase of SWR persistence, but the opposite occurred for F_V. In contrast with sandy loam, fingers in clay loam were shorter and wider, and the SI was the lowest in the four treatments. The SI decreased from 17.1 to 12.3 as SWR persistence increased in treatments SLWR2, SLWR3, and SLWR3. The higher the SI values, the narrower and longer the fingers, the lower the DI values, and thus the more uniform the finger flow distribution. Treatment SLWR2 had the narrowest and longest finger with the largest SI value. When comparing treatments SLWR2, SLWR3, and SLWR4, it was shown that more severely water-repellent soils had more finger numbers and caused more unevenly distributed fingers.

Table 3. Relationship between wetting area (WA) and cumulative infiltration (CI) for the 10 treatments. All the correlations were significant at the 99% level.

Treatment†	Equation	R^2
CLWET	$WA = 20CI^{1.07}$	0.996
CLWR1	$WA = 6.7CI^{1.4}$	0.971
CLWR2	$WA = 37.6CI^{1.04}$	0.993
CLWR3	$WA = 12.1CI^{1.28}$	0.994
CLWR4	$WA = 14.7CI^{1.67}$	0.985
SLWET	$WA = 11.2CI^{1.11}$	0.979
SLWR1	$WA = 1.1CI^{1.04}$	0.992
SLWR2	$WA = 44.8CI^{0.54}$	0.991
SLWR3	$WA = 42.6CI^{0.43}$	0.980
SLWR4	$WA = 155CI^{0.29}$	0.992

† See Table 2 for treatment abbreviation definitions.

The CV values of SI and DI in the treatments SLWR2, SLWR3, and SLWR4 were 0.26 and 0.87, respectively. Both showed moderate variability. The differences were significant between CLWR4 and SLWR2 for finger number, F_V, and SI, and the differences were also significant between SLWR3 and SLWR4 for finger number, F_V, and SI, but the differences were generally insignificant for FW_h and DI. Rye and Smettem (2017) researched the preferential flow channels generated in uniform structure soils with three different SWR persistence values (low, medium and high repellency). Soil tanks were put in the fields to simulate the natural field condition and the wetting patterns after rainfall. They found that the maximum pathway depth of fingers in highly repellent soils (six fingers with 0.25–0.40 cm) was less than that of fingers in medium-repellent soils (six fingers with 0.12–0.25 cm). This result showed that higher SWR did not necessarily generate deeper flow pathways in field tanks. Both this research and Rye and Smettem (2017) showed that the SWR only partially contributes to finger flow development.

The parameter FW_h was nearly constant; however, the parameter F_L is distinctively representative in characterizing finger flow. Therefore, it is necessary to compare the relationship between different finger-related parameters including WA and F_L. Figure 5 demonstrates the variations in F_L vs. time and WA vs. F_L for treatments CLWR4, SLWR2, SLWR3, and SLWR4. Consistent increase of F_L with the increasing time and of WA with the increasing F_L were observed. With the increasing SWR persistence, the increase of WA and F_L could be correlated with time with a power function (Table 5). The F_L and WA were described with a power function with $0.86 < R^2 < 0.99$, which indicated that longer infiltration resulted in longer fingers. However, the increase of WA became slower with the infiltration progress. As the infiltration continued, the development of F_L and WA was limited. Wang et al. (2018) found that this is more complex for layered water-repellent soils. There was certainly some quantitative relationship between F_L and WA, but whether it is linear or not depends on the soil types and layered conditions.

Distribution of Volumetric Soil Water Content

Figure 6 illustrates θ_v distribution along the profiles for the 10 treatments. For both soil textures, the ranges of θ_v tended to be narrower, and the average θ_v was smaller when the water-repellent persistence increased. The θ_v decreased with increasing SWR persistence, which implied greater risk of producing runoff for severely SWR soils. For clay loam soils, θ_v was nonuniformly distributed because of the SWR and occurrence of fingers. In treatment CLWET, θ_v decreased with the soil depth regularly. However, in the other four water-repellent treatments, along with the unstable water movement, the distribution of θ_v was nonuniform. For treatments SLWR2, SLWR3, and SLWR4, when finger flow occurred, the contours maps of θ_v agreed well with the wetting front shapes. Wallach and Jortzick (2008) found that the finger-like wetting fronts presented during point-source infiltration in the wettable and water-repellent sands exhibit soil moisture redistribution mainly in the vertical direction, leaving a wet region at the location of the plume tip where redistribution starts. Ritsema and Dekker (1994) reported that the wettest zone of fingers was at the top in the field soils. In this research, θ_v was higher in the central area near the finger top and decreased to the finger edge, especially in treatment CLWR4, which was

Table 4. The characteristic parameters of finger number, finger length (F_L), width of half finger length (FW_h), finger front velocity (F_v), shape index (SI), and distributing index (DI) for the treatments of CLWR4, SLWR2, SLWR3 and SLWR4 (see Table 2 for treatment abbreviation definitions). No obvious fingers were observed for the other treatments. The statistical differences of the parameters between different treatments were analyzed with an ANOVA using the SPSS 17.0 at a significant level of 0.05.

Treatment	Finger no.	F_L			FW_h			F_v			SI	DI
		Min.	Avg.	Max.	Min.	Avg.	Max.	Min.	Avg.	Max.		
		cm						cm min^{-1}				
CLWR4	1 ± 0b†	–	29 ± 5.7a	–	–	15.2 ± 4a	–	0.3 ± 0.1b	0.5 ± 0.2b	0.7 ± 0.2b	1.9 ± 0.1c	–
SLWR2	2 ± 1ab	28 ± 4.2a	39 ± 11.2a	36 ± 2.8b	1.6 ± 0.4a	2.3 ± 0.7b	3.1 ± 1.2a	1 ± 0.3a	2.2 ± 0.5a	4.5 ± 1.8a	17.1 ± 2.2a	1.6 ± 0.8a
SLWR3	3 ± 1a	33.3 ± 5a	39.2 ± 2.2a	43.7 ± 1.2a	2.7 ± 0.8a	3.1 ± 0.6b	3.4 ± 0.5a	0.9 ± 0.3ab	2.2 ± 0.6a	4.4 ± 1.7a	12.5 ± 1b	1.9 ± 0.5a
SLWR4	3 ± 0a	38 ± 7.8a	41.9 ± 3.8a	45.7 ± 3.1a	3 ± 0.8a	3.5 ± 0.6b	4.0 ± 1.9a	0.6 ± 0.4ab	1.5 ± 0.6ab	2.6 ± 1.4ab	12.3 ± 2.3b	1.8 ± 0.8a

† If lowercase letters are the same, values are not statistically different.

different from Ritsema and Dekker (1994), and this may be due to differences in soil texture and SWR persistence.

Corresponding to Fig. 6, the maximum and CV values of θ_v (based on three replications) are presented in Table 6. The SEs were small. Generally, the θ_v displayed moderate variability. However, the variability of θ_v was not completely associated with SWR persistence. For clay loam soil, CV value increased with the increasing water repellency persistence. In treatments CLWR4 and SLWR2 with fingers, variability of θ_v was prominent, indicating that SWR and finger flow may have resulted in uneven water distribution.

Preferential finger flow commonly forms in water-repellent soils, either homogeneously textured or layered (Carrillo et al., 2000a, 2000b; Wang et al., 2018). The unstable finger flow and the preferential paths lead to earlier arrival to groundwater and increased solute leaching (Larsson et al., 1999). Contamination of wastewater and pesticide would be accelerated when preferential flow occurs frequently. Sandy loam soil, in spite of the same SWR persistence, had more defined effects on production of preferential flow paths than the clay loam soils. The coarser soil texture tended to generate finger flow more easily, as the wetting front was not as uniform as clay loam soils. The larger pores and the uneven microscopic distribution in coarser soils may lead to unstable soil water flow.

The CI, *I*, and WA (vs. time) were consistent for certain SWR persistence and soil texture conditions. The wetting front, finger-related indices (F_L, FW_h, F_v, velocity of finger bottom, SI, and DI), and soil moisture showed more random variations in three replications. These results imply that more replications may be needed in future preferential flow research.

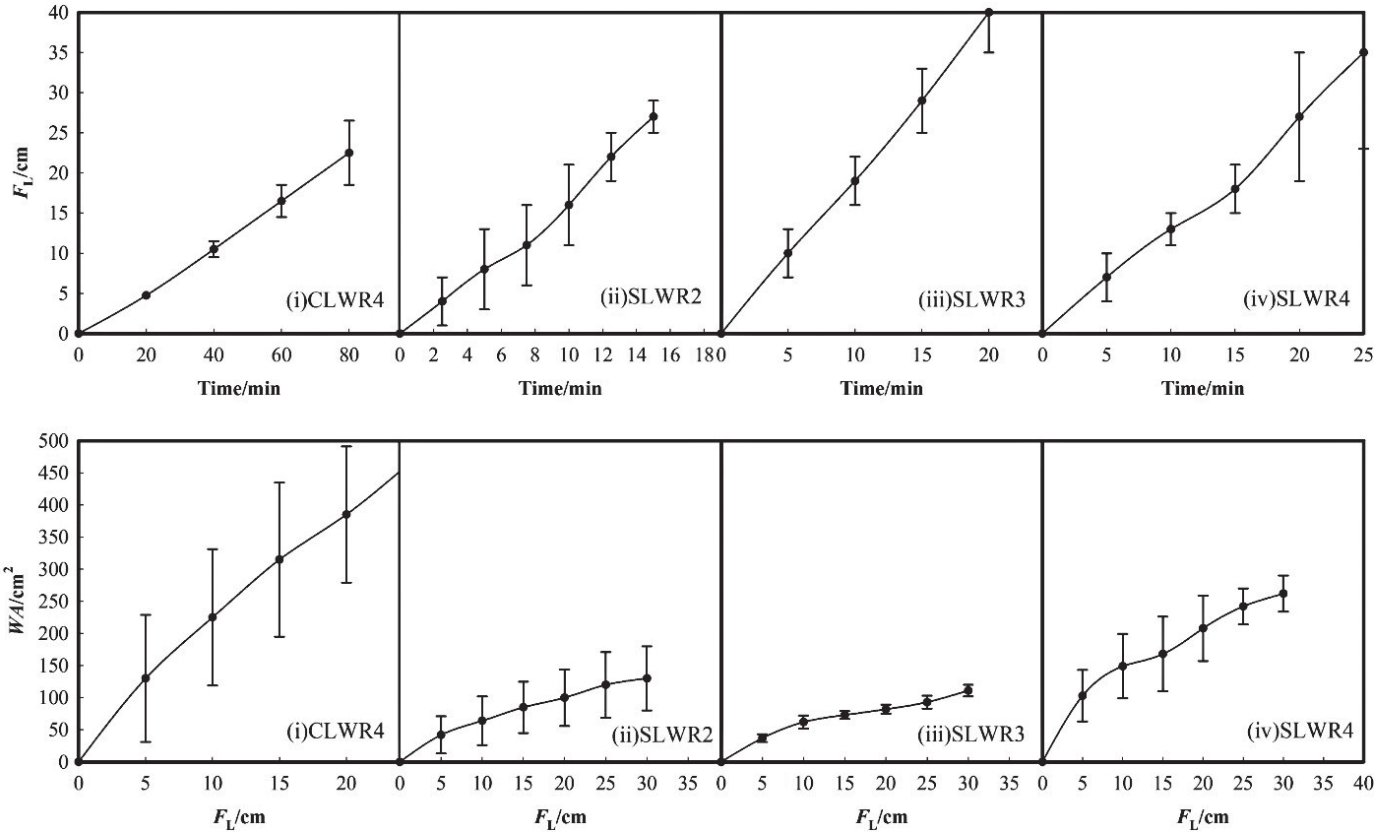

Fig. 5. The variation of finger length (F_L) vs. time (t) and the relationship between cumulative area (WA) and finger length (F_L) for the treatments CLWR4, SLWR2, SLWR3, and SLWR4 (see Table 2 for treatment abbreviation definitions) based on three replications.

Table 5. The fitted equations for wetting area (WA) vs. time (t), finger length (F_L) vs. t, and WA vs. F_L. All the correlations were significant at the 99% level.

Treatment†	Equation	R^2	Equation	R^2	Equation	R^2
CLWR4	$WA = 34.3t^{0.62}$	0.983	$F_L = 0.16t^{1.12}$	0.999	$WA = 36.2F_L^{0.79}$	0.994
SLWR2	$WA = 38.4t^{0.55}$	0.998	$F_L = 1.45t^{1.06}$	0.992	$WA = 14.9F_L^{0.64}$	0.991
SLWR3	$WA = 25.9t^{0.55}$	0.996	$F_L = 1.98t^{0.995}$	0.998	$WA = 15.3F_L^{0.57}$	0.990
SLWR4	$WA = 66.0t^{0.36}$	0.998	$F_L = 1.36t^{0.99}$	0.989	$WA = 44.0F_L^{0.52}$	0.989

† See Table 2 for treatment abbreviation definitions.

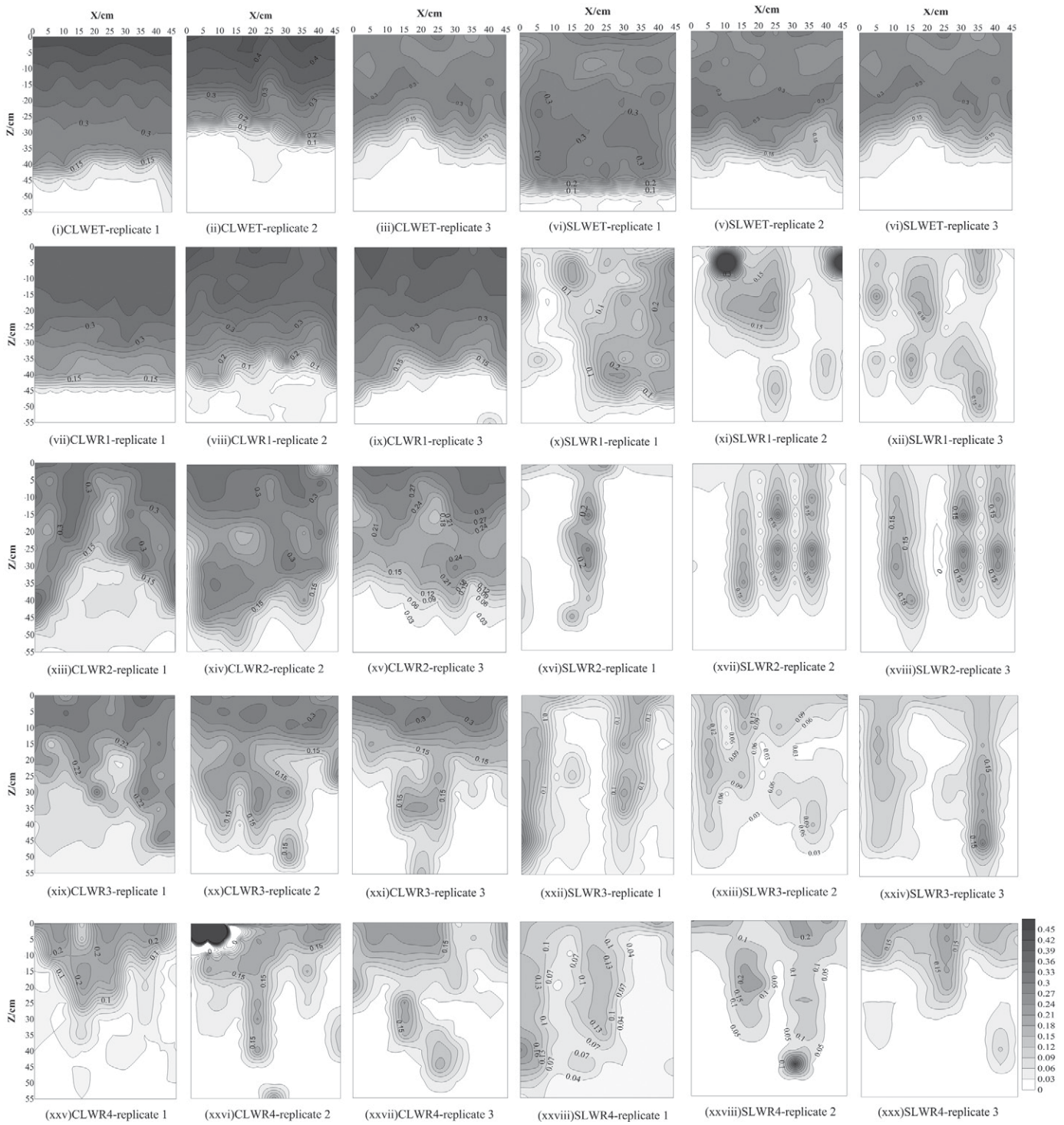

Fig. 6. Contour maps of soil water content (θ_v) for the 10 water-repellent treatments based on three replicates. *X* is the horizontal axis and *Z* is the vertical axis.

Conclusions

The infiltration, wetting front advances, and finger flow development in water-repellent clay loam and sandy loam soils behaved differently than in wettable soil equivalents. The CI decreased as the SWR persistence increased for both soil textures. The wetting fronts became more irregular and unstable as the SWR persistence increased. Finger flow occurred in extremely water-repellent clay loam and in strongly, severely, and extremely water-repellent sandy loam treatments. The finger flow properties (including F_L, FW_h, F_v, SI, and DI) varied when SWR persistence of soils changed. The SI and DI showed irregularity in finger development patterns. The maximum values of SI and DI appeared in

Table 6. The maximum and CV values of soil water content (θ_v) for the 10 different treatments for the clay loam and sandy loam soils based on the three replicates of the 10 treatments.

Treatment†	Max.	CV	Variability level
CLWET	0.45 ± 0.02	0.41	Moderate
CLWR1	0.40 ± 0.02	0.59	Moderate
CLWR2	0.38 ± 0.02	0.62	Moderate
CLWR3	0.36 ± 0.03	0.68	Moderate
CLWR4	0.24 ± 0.02	1.15	Strong
SLWET	0.34 ± 0.02	0.50	Moderate
SLWR1	0.29 ± 0.01	0.73	Moderate
SLWR2	0.33 ± 0.03	1.40	Strong
SLWR3	0.30 ± 0.01	0.97	Moderate
SLWR4	0.28 ± 0.02	0.75	Moderate

† See Table 2 for treatment abbreviation definitions

strongly and extremely water-repellent sandy loam soils, indicating the most irregular fingers. The variations in the finger flow properties and the wetting front movement were obviously different between wettable and water-repellent treatments. There were strong correlations between CI and WA. In the treatments where finger flow occurred (CLWR4, SLWR2, SLWR3, and SLWR4), the power function fit well between F_L and WA. The maximum θ_v increased with the SWR persistence for clay loam soil. The θ_v variability was mostly moderate, but the variability coefficients of treatments for clay loam soils increased with the increase of SWR persistence. In conclusion, soil water movement and finger flow development were affected by SWR persistence; however, the effects of soil texture caused variability in finger flow development. Finger flow development occurs more frequently in the water-repellent sandy loam soils than in water-repellent clay loam soils due to faster flow through coarser textured soil and less time for the breakdown of water repellency.

Acknowledgments

This study was financially supported by the Natural Science Foundation of China (no. 51579213) and the China 111 Project (no. B12007). We are grateful to have received many helpful reviewer comments, which improved the quality of the paper.

References

Bachmann, J., and R.R. van der Ploeg. 2002. A review on recent developments in soil water retention theory: Interfacial tension and temperature effects. J. Plant Nutr. Soil Sci. 165:468–478. doi:10.1002/1522-2624(200208)165:4<468::AID-JPLN468>3.0.CO;2-G

Bauters, T.W.J., T.S. Steenhuis, J.Y. Parlange, and D.A. Dicarlo. 1998. Preferential flow in water-repellent sands. Soil Sci. Soc. Am. J. 62:1185–1190. doi:10.2136/sssaj1998.03615995006200050005x

Bisdom, E., L.W. Dekker, and J.F.T. Schoute. 1993. Water repellency of sieve fractions from sandy soils and relationships with organic material and soil structure. Geoderma 56:105–118. doi:10.1016/0016-7061(93)90103-R

Carrillo, M.L.K., J. Letey, and S.R. Yates. 2000a. Unstable flow in a layered soil: I. The effects of a stable water-repellent layer. Soil Sci. Soc. Am. J. 64:450–455. doi:10.2136/sssaj2000.642450x

Carrillo, M.L.K., J. Letey, and S.R. Yates. 2000b. Unstable water flow in a layered soil: II. Effects of an unstable water-repellent layer. Soil Sci. Soc. Am. J. 64:456–459. doi:10.2136/sssaj2000.642456x

de Rooij, G.H. 2000. Modeling fingered flow of water in soils owing to wetting front instability: A review. J. Hydrol. 231–232:277–294. doi:10.1016/S0022-1694(00)00201-8

DeBano, L. F. 1981. Water repellent soils: A state-of-the-art. General Tech. Rep. PSW-46. USDA For. Serv., Pacific Southwest For. Range Exp. Stn., Berkeley, CA. doi:10.2737/PSW-GTR-46

Dekker, L.W., and P.D. Jungerius. 1990. Water repellency in the dunes with special reference to the Netherlands. Catena Suppl. 18:173–183.

Dekker, L.W., and C.J. Ritsema. 1994. How water moves in a water repellent sandy soil: 1. Potential and actual water repellency. Water Resour. Res. 30:2507–2517. doi:10.1029/94WR00749

Deurer, M., and J. Bachmann. 2007. Modeling water movement in heterogeneous water-repellent soil: 2. A conceptual numerical simulation. Vadose Zone J. 6:446–457. doi:10.2136/vzj2006.0061

Ganz, C., J. Bachmann, A. Lamparter, S.K. Woche, W.H.M. Duijnisveld, and M.O. Göbel. 2013a. Specific processes during in situ infiltration into a sandy soil with low-level water repellency. J. Hydrol. 484:45–54. doi:10.1016/j.jhydrol.2013.01.009

Ganz, C., J. Bachmann, U. Noell, W.H. Duijnisveld, and A. Lamparter. 2013b. Hydraulic modeling and in situ electrical resistivity tomography to analyze ponded infiltration into a water repellent sand. Vadose Zone J. 13:246–250. doi:10.2136/vzj2013.04.0074

Goebel, M., S.K. Woche, J. Bachmann, A. Lamparter, and W.R. Fischer. 2007. Significance of wettability-induced changes in microscopic water distribution for soil organic matter decomposition. Soil Sci. Soc. Am. J. 71:1593–1599. doi:10.2136/sssaj2006.0192

Hardie, M.A., W.E. Cotching, R.B. Doyle, G. Holz, S. Lisson, and K. Mattern. 2011. Effect of antecedent soil moisture on preferential flow in a texture-contrast soil. J. Hydrol. 398:191–201. doi:10.1016/j.jhydrol.2010.12.008

Kramers, G., J.C. van Dam, C.J. Ritsema, F. Stagnitt, K. Oostindie, and L. Dekker. 2005. A new modelling approach to simulate preferential flow and transport in water repellent media: Parameter sensitivity, and effects on crop growth and solute leaching. Aust. J. Soil Res. 43:371–382. doi:10.1071/SR04098

Larsson, M.H., N.J. Jarvis, G. Torstensson, and R. Kasteel. 1999. Quantifying the impact of preferential flow on solute transport to tile drains in a sandy field soil. J. Hydrol. 215:116–134. doi:10.1016/S0022-1694(98)00265-0

Li, Y., X. Ren, R. Hill, R. Malone, and Z. Ying. 2018. Characteristics of water infiltration in layered water repellent soils. Pedosphere 28:775–792. doi:10.1016/S1002-0160(17)60414-4

Li, Y., W. Wang, and X. Hu. 2013. Numerical simulation of soil water infiltration under bubbled root irrigation based on HYDRUS-3D. (In Chinese.) J. Drain. Irrig. Mach. Eng. 31:346–552. doi:10.3969/j.issn.1674-8530.2013.06.017

Li, Y., X.F. Wang, Z.K. Cao, and B.C. Si. 2017. Water repellency as a function of soil water content or suction influenced by drying and wetting processes. Can. J. Soil Sci. 97:226–240.

Nielsen, D.R., and J. Bouma, editors. 1985. Soil spatial variability: Proceedings of a Workshop of the ISSS and the SSSA, Las Vegas, NV. 30 Nov.–1 Dec. 1984. Pudoc, Wageningen, the Netherlands.

Rezanezhad, F., H.J. Vogel, and K. Roth. 2006. Experimental study of fingered flow through initially dry sand. Hydrol. Earth Syst. Sci. 3:2595–2620. doi:10.5194/hessd-3-2595-2006

Ritsema, C.J., and L.W. Dekker. 1994. How water moves in a water repellent sandy soil. 2. Dynamics of fingered flow. Water Resour. Res. 30:2519–2531. doi:10.1029/94WR00750

Ritsema, C.J., and L.W. Dekker. 2000. Preferential flow in water repellent sandy soils: Principles and modeling implications. J. Hydrol. 231–232:308–319. doi:10.1016/S0022-1694(00)00203-1

Ritsema, C.J., L.W. Dekker, J.L. Nieber, and T.S. Steenhuis. 1998. Modeling and field evidence of finger formation and finger recurrence in a water repellent sandy soil. Water Resour. Res. 34:555–567. doi:10.1029/97WR02407

Ritsema, C.J., L.W. Dekker, E.G.M. van den Elsen, K. Oostindie, T.S. Steenhuis, and J.L. Nieber. 1997. Recurring fingered flow pathways in a water repellent sandy field soil. Hydrol. Earth Syst. Sci. 1:777–786. doi:10.5194/hess-1-777-1997

Robichaud, P.R., J.W. Wagenbrenner, F.B. Pierson, K.E. Spaeth, L.E. Ashmun, and C.A. Moffet. 2016. Infiltration and interrill erosion rates after a wildfire in western Montana, USA. Catena 142:77–88. doi:10.1016/j.catena.2016.01.027

Rye, C.F., and K.R.J. Smettem. 2017. The effect of water repellent soil surface layers on preferential flow and bare soil evaporation. Geoderma 289:142–149. doi:10.1016/j.geoderma.2016.11.032

Sepehrnia, N., H.M. Ali, A. Majid, and L. L'ubomír. 2017. Soil water repellency changes with depth and relationship to physical properties within wettable and repellent soil profiles. J. Hydrol. Hydromech. 65:99–104. doi:10.1515/johh-2016-0055

Song, E.Z., J.G. Schneider, S.H. Anderson, K.W. Goyne, and X. Xiong. 2014. Wetting agent influence on water infiltration into hydrophobic sand: II. Physical properties. Agron. J. 106:1879–1885. doi:10.2134/agronj14.0153

SPSS. 2008. SPSS Statistics for Windows. Version 17.0. SPSS, Chicago.

Systat Software. 2013. SigmaPlot software. Release 12.5. Systat Softw., San Jose, CA.

Urbanek, E., and S.H. Doerr. 2017. CO_2 efflux from soils with seasonal water repellency. Biogeosciences 14:4781–4794 doi:10.5194/bg-14-4781-2017

Wallach, R., and C. Jortzick. 2008. Unstable finger-like flow in water-repellent soils during wetting and redistribution: The case of a point water source. J. Hydrol. 351:26–41. doi:10.1016/j.jhydrol.2007.11.032

Wang, Y., Y. Li, X. Wang, and H.W. Chau. 2018. Finger flow development in layered water-repellent soils. Vadose Zone J. 17:170171. doi:10.2136/vzj2017.09.0171

Wang, Z., Q.J. Wu, L. Wu, C.J. Ritsema, L.W. Dekker, and J. Feyen. 2003. Effects of soil water repellency on infiltration rate and flow instability. J. Hydrol. 231:265–276.

Zhang, J.F. 2004. Experimental study on infiltration characteristics and finger flow in layer soils of the loess area. Ph.D. diss. Northwest A&F Univ., Yangling, China.

Zheng, S., S.D.N. Lourenço, P.J. Cleall, T.F.M. Chui, A.K.Y. Ng, and S.W. Millis. 2017. Hydrologic behavior of model slopes with synthetic water repellent soils. J. Hydrol. 554:582–599. doi:10.1016/j.jhydrol.2017.09.013.